Plant Soil (2017) 417:43–52
DOI 10.1007/s11104-017-3233-x

REGULAR ARTICLE

Depth profiles of soil carbon isotopes along a semi-arid grassland transect in northern China

Chao Wang · Haiwei Wei · Dongwei Liu · Wentao Luo · Jianfeng Hou · Weixin Cheng · Xingguo Han · Edith Bai

Received: 21 November 2016 / Accepted: 21 March 2017 / Published online: 4 April 2017
© Springer International Publishing Switzerland 2017

Abstract

Background Soil is an important organic carbon (C) pool in terrestrial ecosystems, but knowledge on soil organic carbon (SOC) decomposition rate and influencing factors remains limited, particularly in arid and semi-arid grasslands. Models show that global semi-arid regions are experiencing more extreme climate events, which may trigger more C loss from soils.

Methods We used the stable carbon isotope ($\delta^{13}C$) of plant and soil depth profile to examine decomposition rates of SOC along a 2200 km semi-arid grassland transect in northern China. Beta (β) was calculated from the relationship between $\delta^{13}C$ and C concentrations of plant and soil profile (0–100 cm). Partial correlation analysis and structure equation models were used to analyze correlations between beta and climatic and edaphic variables.

Results We found that the $\delta^{13}C$ values increased from plant tissues to surface soil and then deep soil at all sites, while the SOC concentration decreased. The β values ranged from −0.33 to −2.27, with an average value at −1.37. There was a positive correlation between β value and SOC decomposition rate constant (k), supporting the hypothesis that enrichment of $\delta^{13}C$ along soil depth profile was mainly due to isotopic fractionation during microbial SOC decomposition. The correlation between β value and aridity index was mainly due to the variations of edaphic properties such as soil C/N ratio with aridity index, pointing to the more important role of edaphic properties in β value than climatic factors.

Conclusions Despite uncertainties associated with the interpretation of soil $\delta^{13}C$ along its depth profile, our results demonstrated that soil $\delta^{13}C$ could provide an independent benchmark for examining model-based predictions of SOC decomposition in semi-arid grasslands. Incorporation of both climatic and edaphic variables into models may enhance the predictions for SOC dynamics under global climate changes.

Keywords Soil organic carbon · Turnover rate · Beta value · Carbon decomposition · Aridity index · Grasslands · Climate change models

Responsible Editor: Ingrid Koegel-Knabner.

Electronic supplementary material The online version of this article (doi:10.1007/s11104-017-3233-x) contains supplementary material, which is available to authorized users.

C. Wang · H. Wei · D. Liu · W. Luo · J. Hou · W. Cheng · X. Han · E. Bai (✉)
CAS Key Laboratory of Forest Ecology and Management, Institute of Applied Ecology, Chinese Academy of Sciences, Shenyang 110164, China
e-mail: baie@iae.ac.cn

H. Wei · J. Hou
College of Resources and Environment, University of Chinese Academy of Sciences, Beijing 100049, China

W. Cheng
Department of Environmental Studies, University of California, Santa Cruz, 1156 High Street, Santa Cruz, CA 95064, USA

Abbreviations

N	Nitrogen
C	Carbon
SOC	Soil organic carbon
SOM	Soil organic matter
MAP	Mean annual precipitation
MAT	Mean annual temperature
AI	Aridity index
PET	Potential evaportranspiration
SEMs	Structure equation models

Introduction

Semi-arid grasslands occupy a substantial proportion of terrestrial cover and are significant components of global biogeochemical cycles (Delgado-Baquerizo et al. 2013; Reynolds et al. 2007). Specifically, the soils in semi-arid grasslands store about 15% of global organic carbon (C) (Anderson 1991; Lal 2004), which may be more sensitive to changing precipitation regimes under global climate change because drying/wetting cycles may trigger a rapid pulse of soil biological activity and thereby influencing soil C cycling (Dijkstra et al. 2012; Nielsen and Ball 2015; Reed et al. 2012). However, the reliable gauge of soil organic carbon (SOC) decomposition rate and its controlling factors remains the challenging tasks, especially in the semi-arid grasslands. In addition, most studies on SOC decomposition only focus on surface soils, while more studies recognize that deep soils (> 50 cm) also contain large amount of C which could also be decomposed over time (Fontaine et al. 2007). An integrated estimation of SOC decomposition rate along the whole soil profile could help us better understand and predict reactions of SOC to changing climate.

The stable carbon isotopic composition ($\delta^{13}C$) in soil has been considered as an integrative measure of SOC decomposition (Bird et al. 1996), and therefore it could be a potential approach for understanding soil C dynamics across regional and global scales (Nadelhoffer and Fry 1988; Staddon 2004). Because most soil organic matter (SOM) originates from plant residues, soil $\delta^{13}C$ reflects its plant tissue sources and the subsequent processes within the soil (Ehleringer et al. 2000; Schweizer et al. 1999). It is widely observed that $\delta^{13}C$ of SOC varied with soil depth profile (Accoe et al. 2002; Brunn et al. 2014; Garten et al. 2000; Powers and Schlesinger 2002). Subsurface SOC generally is enriched with $\delta^{13}C$ up to several parts per thousand than C in aboveground plant litter inputs, the O horizon and surface mineral SOM, concomitantly with decreasing SOC concentration (Fig. S1). The commonly held hypothesis associated with this pattern of soil $\delta^{13}C$ is that microbes prefer the lighter ^{12}C during the formation of soil organic matter and leave the heavier ^{13}C in the solid substrate, producing more enriched $\delta^{13}C$ with soil vertical profiles. These trends result in negative linear correlation between the log-transformed SOC concentration and soil $\delta^{13}C$ (Acton et al. 2013; Garten et al. 2000; Garten and Hanson 2006; Powers and Schlesinger 2002). The slope of the linear regression (i.e. β value) between soil $\delta^{13}C$ and the log-transformed SOC concentration has been considered as a proxy of SOC decomposition rates (Garten et al. 2000; Kohl et al. 2015; Poage and Feng 2004). However, few studies have provided direct evidence of correlation between β values and soil SOC decomposition rates. Of course, the Suess effect (the mixture of anthropogenic, isotopically depleted CO_2 caused the decrease in atmospheric $\delta^{13}C$-CO_2) (Boström et al. 2007) and the mixing of different C sources (Acton et al. 2013; Diochon and Kellman 2008) may also cause the increasing pattern of soil $\delta^{13}C$ with depth. Therefore, it is important to identify which mechanism explains the most of the variation of soil $\delta^{13}C$ with depth in order to use $\delta^{13}C$ of SOC effectively to study SOM decomposition.

Empirical studies have identified factors which regulate β values, including climatic factors, e.g. temperature (Campbell et al. 2009; Garten et al. 2000), precipitation (Acton et al. 2013) and soil properties (Wynn et al. 2006). However, most of these studies were conducted in temperate and tropical forests, with limited coverage of arid and semi-arid grasslands (Acton et al. 2013; Powers and Schlesinger 2002). Arid and semi-arid grasslands are characterized with low precipitation with pulse rainfall events, and microorganisms in those soils may be more sensitive to environmental changes, resulting in more C losses than forest soils (Carvalhais et al. 2014). The biogeochemical cycling processes in arid and semi-arid areas may be driven by different biotic and abiotic factors from other ecosystems (Feng et al. 2016; Luo et al. 2016). Whether the soil $\delta^{13}C$ depth profiles and β values observed in forests still hold true in arid grasslands still needs to be explored.

In this study, we investigated $\delta^{13}C$ signatures of plant and soil depth profile at 27 sites along a 2200 km semi-arid grassland in northern China (Fig. S2). The slope (β value) of linear relationship between $\delta^{13}C$ and logarithm of plant leaf and soil in top meter of soil depth profile was calculated. We hypothesized that (1) soil $\delta^{13}C$

increases with depth profile for each study site along the grassland transect; (2) microbial ^{13}C discrimination during SOC decomposition is the dominant mechanism causing increasing $\delta^{13}C$ with depth and consequently β value would be positively correlated with SOM mineralization rate; and (3) β value would correlate with climatic and edaphic factors, reflecting their potential effects on SOM mineralization. This study could then provide clues on soil carbon dynamics in semi-arid regions and the potential feedbacks to climatic changes.

Material and methods

Study sites

Study areas were located in the Inner Mongolia grasslands in northern China. We selected a 2200 km grassland transect from east to west across the whole study region, which covered approximately 24° ranging from 96°40′ E to 120°28′ E and with latitude ranging from 39°51′ N to 50°30′ N (Fig. S2). Elevation declines from about 1200 m in the west to approximately 600 m in the east. However, the topography is muted, with tablelands and gently rolling hills (Feng et al. 2016). The climate is predominantly arid and semi-arid continental; the mean annual precipitation (MAP) ranges from 90 mm to 420 mm and mean annual temperature (MAT) ranges from −2 °C to +7 °C. Along this east-west climate gradient, the study areas cover three vegetation types: desert steppe, typical steppe and meadow steppe (Wang et al. 2016; Wang et al. 2014). The parent material of soils is formed primarily since early Holocene. Soils can be classed into Haplic Calcisols, Calcic Cambisols and Calcic Kastanozems from west to east (Feng et al. 2016). The Haplic Calcisols were in an initial stage of soil formation, where calcium carbonate accumulated on the soil surface and lacked a calcic horizon. The Calcic Cambisols developed a minimal B horizon. At the wetter sites, Calcic Kastanozems were well developed with secondary (pedogenic) carbonate accumulation at depth. The calcium oxide accumulated in subsurface horizons to 20–50 cm for Calcic Cambisols and >40 cm for Calcic Kastanozems (Feng et al. 2016).

Soil and plant sampling

We conducted the field sampling campaign during July and August in 2012, and a total of 27 locations (number from 1 to 27) were selected with a mean interval of 60 km (Fig. S2). At each location (predominant by C_3 plants), two large plots (50 m × 50 m) at a distance of less than 2 km were setup first and then five 1 m × 1 m sub-plots were selected at each corner and the center of each large plot. In each 1 m × 1 m sub-plot, every species was identified, chipped at the ground level and pooled for aboveground biomass calculation. Then twenty soil cores in each 1 m × 1 m sub-plot were collected and divided into 0–10 cm, 10–20 cm, 20–40 cm, 40–60 cm and 60–100 cm depth segments and bulked to form one composite sample for each segment per sub-plot. Finally, each sampling site had ten soil replicates.

For plant samples, two dominant grass genera (*Stipa*, *Leymus*) and three shrub genera (*Caragana*, *Reaumuria* and *Salsola*) were selected for isotope analyses. For *Stipa*, and *Leymus*, we sampled both leaves and roots (0–30 cm soil depth). Plant leaf and root samples were washed with deionized water to remove dust particles and then dried at 65 °C for 48 h for further analyses.

Laboratory analyses

Soil sub-samples were sieved through a 2 mm sieve and dried at 65 °C. Both plant and soil samples were ground in a ball mill and then stored in a plastic bag until further analysis. Following the method described by Harris et al. (2001), all soil samples were washed using 10–50 mL of 0.5 M HCl to remove carbonate and washed twice with distilled water before carbon elemental and isotopic composition analysis. Another balled soil sub-sample without HCl washing treatment was used to analyze total N concentration. All analyses for SOC, total N concentration and C isotope ratios were carried out at the Stable Isotope Faculty of University of California, Davis. About 3 mg of leaf and root samples and 20 mg of soil samples were loaded into a capsule and determined using an Elementar Vario EL Cube (Elementar Analysis system GmbH, Hanau, Germany) interfaced to a PDZ Europa 20–20 isotope ratio mass spectrometer (Sercon Ltd., Cheshire, UK), with an overall precision better than 0.2‰. Isotope value was expressed in parts per thousand (‰) relative to Pee Dee Belemnite (PDB) for $^{13}C/^{12}C$, using standard delta (δ) notion.

To determine the soil microbial respiration, we carried out a 21-day-long soil C decomposition experiment in laboratory. 100 g of air-dried soil was placed in a polypropylene column (2 cm in diameter, 30 cm in height) and water holding capacity (WHC) was adjusted

to 60%. The CO_2 accumulated in the polypropylene column during the incubation was sampled and then measured by an infrared CO_2 analyzer (LiCOR 6262, Lincoln, NB, USA). Soil water content was maintained at 60% WHC throughout the incubation by daily addition of deionized water as necessary.

A sub-sample soil sieved through a 2.0 mm screen (10 g) was used for pH value in water at a 1: 2.5 soil/water ratio and another sub-sample was fractionated into sand (particle size, 50–300 μm), silt (2–50 μm), and clay (< 2 μm) using ultrasonic energy method. All results of particle size analysis were expressed as percentage, by weight, of the oven-dried soil. The concentration of phosphorus (P) determined at 880 nm by molybdate colorimetry on a spectrophotometer. The concentrations of potassium (K), calcium (Ca), magnesium (Mg), copper (Cu), manganese (Mn), iron (Fe) and zinc (Zn) were measured either using inductively coupled plasma mass spectrometry (Perkin Elmer, ELAN-6000) or inductively coupled plasma emission spectroscopy (Perkin Elmer, OPTIMA 3000 DV) (Luo et al. 2016).

Meteorological data

The spatial geographical coordinates and elevation of each sampling location were recorded by GPS (eTrex Venture, Garmin, USA). MAP, MAT and Potential Evapotranspiration (PTE) of each sampling location were calculated from the WorldClim database (Hijmans et al. 2005) using ArcGIS 10.0 Spatial Analysis tool (SERI, Redlands, CA) based on the geographical coordinates (latitude and longitude).

Data analyses

Since the temperature and precipitation covary along the transect, we used aridity index (AI = MAP/PET) to present climatic variable. We made an ordinary least squares (OLS) regression between the logarithm of C concentration and $\delta^{13}C$ in leaves, roots and mineral soils (all five depths) for each site (Fig. S1). The slopes of regression were considered as the β values. Soil decomposition rate constants (k, $yr.^{-1}$) were calculated by dividing measured CO_2 respiration rates in incubation experiment by the corresponding soil carbon concentration. We employed OLS regression analyses to qualify the relationship between β value and k. In addition, bivariate relationships between climatic variables (AI) and $\delta^{13}C$ / β value were estimated using zero-order correlations (with all edaphic variables) and partial correlations by controlling for a single edaphic variable (i.e. clay, silt, pH, N, C/N ratio, P, K, Ca, Mg, Mn, Fe, Zn, Cu) and all variables combined (All). We further used structure equation models (SEMs) to explore primary driving factors on variations of β value. We started the SEMs procedure with the specification of a conceptual model of hypothetical relationships, based on a priori and theoretical knowledge. In the SEMs analysis, we compared the model-implied variance-covariance matrix against the observed variance-covariance matrix. Data were fitted to the models using the maximum likelihood estimation method. For simplicity, the least significant path was deleted and the model was re-estimated; then the next least significant path was removed, and so on, until the paths that remained in the final SEM were all significant. Non-significant χ^2 tests ($p > 0.05$) and CFI values over 0.90 were considered acceptable. The direct and indirect effects were based on SEM which simulates the cause-consequence relations among variables and predicts the direct (significant correlation with beta) and indirect (non-significant correlation with beta) effects statistically considering the inter-correlation among independent variables.

Results

Carbon concentration and $\delta^{13}C$

The leaf carbon concentration of the five genera we sampled ranged from 36.8% to 46.4% with an average at 43.8% (Table S1). On average, leaf $\delta^{13}C$ was −26.6‰, which was 1.5‰ more ^{13}C–depleted than surface soil $\delta^{13}C$ (Table 1). The mean SOC concentration decreased from 1.16% to 0.37% with increasing depth while the mean soil $\delta^{13}C$ values increased from −25.1‰ to −23.1‰ (Table 1 and Table S1). Along this semi-arid grassland transect, the vertical enrichment in $\Delta\delta^{13}C$ ($\Delta\delta^{13}C = \delta^{13}C_{soil\ (100cm)} - \delta^{13}C_{leaf}$) ranged from 0.6‰ to 6.5‰ with an average at 3.7‰ (Table 1).

β values

Ordinary least squares regression of $\delta^{13}C$ with the logarithm of SOC fit the data well for most of the site, as judged by R^2 and P values (Table 1). The estimated regression slopes, i.e. β values, for 27 sites ranged from −0.33 to −2.27 (Table 1). Because lower β value means faster SOC decomposition, we made a negative log-

Table 1 Mean $\delta^{13}C$ values (‰) of leaf, root (0–30 cm) and soil (0–100 cm) at 27 sites along the grassland transect. $\Delta\delta^{13}C = \delta^{13}C_{soil(60\text{-}100cm)} - \delta^{13}C_{leaf}$. Beta (β) values were from linear regressions between log (SOC) and $\delta^{13}C$ (Fig. S1)

Site	Leaf	Root	0–10	10–20	20–40	40–60	60–100	$\Delta\delta^{13}C$	β	ln (−β)	R^2	*P*
1	-26.3	-	−26.1	−22.6	−21.7	−21.6	−21.6	4.3	−1.24	0.22	0.64	0.05
2	−27.4	−25.7	−25.0	−20.3	−22.3	−20.7	−21.6	5.9	−1.93	0.66	0.77	0.01
3	−26.3	−24.6	−25.0	−20.7	−21.4	−20.1	−21.5	4.4	−1.64	0.50	0.69	0.01
4	−26.8	−25.3	−24.4	−20.7	−21.0	−21.3	−20.1	6.3	−2.02	0.70	0.82	0.00
5	−25.8	−24.8	−25.3	−23.3	−22.2	−21.0	−22.0	3.7	−1.21	0.19	0.55	0.05
6	−26.4	−25.2	−23.5	−21.2	−21.7	−20.9	−21.3	5.1	−1.74	0.56	0.79	0.00
7	−26.8	−25.9	−25.3	−23.1	−23.0	−23.5	−24.5	1.9	−1.29	0.26	0.70	0.00
8	−26.6	−25.1	−24.5	−20.2	−20.8	−21.5	−21.6	5.0	−1.92	0.65	0.70	0.02
9	−26.7	−26.1	−24.1	−21.9	−21.7	−20.3	−20.1	6.6	−2.27	0.82	0.78	0.00
10	−25.7	−25.8	−23.4	−21.2	−20.3	−21.1	−20.9	4.9	−1.80	0.59	0.87	0.00
11	−25.5	−25.7	−24.1	−22.6	−21.6	−20.4	−21.2	4.3	−1.52	0.42	0.78	0.00
12	−26.1	−25.5	−23.3	−21.0	−20.6	−20.3	−20.1	6.5	−2.20	0.79	0.91	0.00
13	−26.4	−24.2	−23.5	−20.9	−21.4	−22.3	−23.9	4.5	−1.42	0.35	0.70	0.02
14	−26.2	−24.6	−24.8	−22.6	−23.0	−23.2	−23.8	2.9	−1.36	0.31	0.78	0.01
15	−26.7	−25.2	−23.9	−22.2	−22.7	−23.6	−23.1	3.9	−1.45	0.37	0.75	0.00
16	−27.4	−25.6	−24.3	−23.1	−23.6	−24.8	−24.4	3.4	−1.16	0.15	0.60	0.02
17	−27.1	−25.5	−26.4	−24.4	−24.4	−24.5	−24.4	3.3	−1.02	0.02	0.54	0.03
18	−27.4	−25.6	−25.7	−24.3	−24.1	−25.0	−25.8	1.6	−0.98	−0.02	0.62	0.02
19	−26.7	−26.2	−26.0	−24.9	−25.0	−24.1	−25.2	1.9	−0.93	−0.08	0.62	0.01
20	−27.2	−26.4	−27.1	−24.7	−24.9	−24.7	−24.8	2.3	−1.27	0.24	0.65	0.03
21	−26.7	−26.0	−25.0	−22.6	−22.8	−23.9	−23.6	3.6	−1.54	0.43	0.78	0.00
22	−26.1	−25.9	−25.1	−23.8	−23.8	−21.8	−21.2	4.9	−1.65	0.50	0.61	0.04
23	−26.7	−25.5	−25.8	−23.7	−24.6	−24.2	−24.1	2.9	−0.96	−0.04	0.64	0.01
24	−26.6	−26.6	−25.8	−26.0	−24.3	−25.3	−25.4	2.0	−0.74	−0.30	0.56	0.02
25	−26.1	−26.5	−25.9	−24.5	−25.0	−24.8	−25.1	1.0	−0.73	−0.32	0.68	0.01
26	−27.2	−27.0	−26.6	−26.4	−26.6	−26.1	−26.4	0.6	−0.33	−0.26	0.76	0.00
27	−27.3	−26.6	−27.1	−25.6	−25.6	−25.8	−25.9	1.6	−0.66	−0.41	0.62	0.01
Mean	−26.6	−25.7	−25.1	−22.9	−23.0	−22.8	−23.1	3.7	−1.37	0.23		

transformation for β to make it easier to understand and got ln(−β) ranging between −0.41 and 0.82 with a mean value at 0.23 (Table 1). There was a significantly positive relationship between ln (−β) and soil carbon decomposition rate ln(k), with R^2 at 0.51 (Fig. 1). Besides, a weak relationship was observed between leaf $\delta^{13}C$ and surface soil $\delta^{13}C$ (R^2 = 0.21, $P < 0.01$, Fig. S3). In addition, surface soil $\delta^{13}C$ was positively correlated with ln(−β) along the transect (Fig. S3).

Factors affecting soil $\delta^{13}C$ and ln(−β)

The $\delta^{13}C$ values of surface soils were negatively correlated with AI, soil N, soil C/N, soil silt concentration (Fig. S4) and soil P (Fig. S5) with R^2 at 0.47, 0.43, 0.49, 0.24 and 0.30 respectively. Moreover, soil $\delta^{13}C$ was positively correlated with pH (R^2 = 0.43, $P < 0.01$; Fig. S4) and Fe (R^2 = 0.14, P = 0.05; Fig. S5).

We found that ln (−β) decreased with the increasing AI (R^2 = 0.59, $P < 0.01$; Fig. 2a), soil N (R^2 = 0.38, $P < 0.01$; Fig. 2c), and soil C/N (R^2 = 0.65, $P < 0.01$; Fig. 2d). Positive relationships were observed between ln (−β) and soil pH (R^2 = 0.54, $P < 0.01$; Fig. 2b) as well as soil Cu, Zn, Mg, and Fe (Fig. S6).

Although AI had significant effects on ln (−β) (zero-order, Table 2), partial correlation analysis (n = 270) revealed that the Pearson correlation coefficients between AI and ln (−β) decreased significantly after removing

edaphic variables ('All', Table 2). Furthermore, we built structure equation models (SEMs) to develop the paths between climatic and edaphic variables and ln (−β) (Fig. S7). The final SEMs revealed that AI had predominately indirect effect on ln (−β) via their influence on soil C/N ratio (Fig. 3 and Table S2).

Discussion

Our results showed that $\delta^{13}C$ increased along soil depth profile at all semi-arid grassland sites (Table 1), which supported our hypothesis (1) and agreed with the widely reported phenomenon of enrichment of soil $\delta^{13}C$ with increasing soil depth (Accoe et al. 2002; Boström et al. 2007; Garten et al. 2000; Nadelhoffer and Fry 1988; Powers and Schlesinger 2002). Mean $\delta^{13}C$ enrichment in our semi-arid grassland soil was 3.7‰, which was lower than the observations in Costa Rica rain forest (5.9‰) (Powers and Schlesinger 2002) and Amazonian forest (5.0‰) (Desjardins et al. 1994), but higher than that in a temperate mature beech (3.4‰) (Brunn et al. 2014) and a boreal forest (1.2‰) (Flanagan et al. 1996). This difference in the enrichment of soil $\delta^{13}C$ with depth may be attributed to the differences of the quality and quantity of aboveground plant C inputs and the consequences of C cycling processes in soil depth profiles.

As summarized in the introduction, several processes have been proposed to explain the $\delta^{13}C$ enrichment with increasing soil depth (Ehleringer et al. 2000; Garten et al. 2000; Wynn et al. 2006). Average $\delta^{13}C$ of atmospheric CO_2 has been decreasing from −6.5‰ to −7.8% since the industrial revolution owing to the combustion of ^{13}C–depleted fossil fuel and biomass burning (Friedli et al. 1987). Therefore, this Suess effect could have caused the pattern of increasing $\delta^{13}C$ with depth because deeper soil is older and less affected by changing $\delta^{13}C$ of atmospheric CO_2 (Wynn et al. 2006). However, the decrease in $\delta^{13}C$-CO_2 was smaller (i.e., 1.4–1.5‰) than the average decrease of $\delta^{13}C$ along our grassland transect (3.7‰), pointing to other mechanisms besides the Suess effect. In addition, Torn et al. (2002) showed that the $\delta^{13}C$ profiles of a modern soil and its 100-year-old archive soil from the same site were similar, indicating that the gradient of soil $\delta^{13}C$ with depth was not due to depletion of atmospheric $^{13}CO_2$ by fossil fuel combustions.

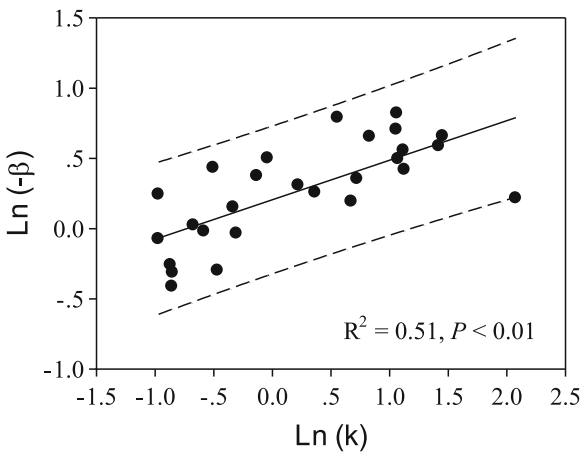

Fig. 1 Relationship between ln(−β) and soil carbon decomposition rate (k)

Second, different SOM sources and mixing effects may contribute to the enrichment of $\delta^{13}C$ along soil depth (Acton et al. 2013; Garten et al. 2000). Many studies showed that $\delta^{13}C$ value of plant roots was generally more enriched than leaf from the same plant (Garten et al. 2000; Powers and Schlesinger 2002). Therefore, if deep soil C mainly came from root litter while leaf and stem derived litter contributed more to surface soils, the $\delta^{13}C$ pattern of SOC should increase with depth (Wynn et al. 2006). Of course, root litter may contribute more than leaf litter to surface soil instead, nullifying this assumption and thereby minimizing the possibility of this mechanism underlying the enrichment of $\delta^{13}C$ along soil depth. Another research conducted by Kohl et al. (2015) suggested that increased proportions of soil bacteria (^{13}C enriched) relative to fungi (^{13}C depleted) biomass with depth may also contribute to increasing $\delta^{13}C$ with depth via contributions from "necromass" to SOC. However, the contribution from microbial debris or vegetation tissues to variations of $\delta^{13}C$ of SOC is still difficult to assess. The carbon isotopic signature of different SOM sources may mix and offset each other, causing no significant change of $\delta^{13}C$ along the soil depth profile. Besides, the proportion of carbonate in total carbon was difference among sites, which may influence soil aggregate and then affect soil organic carbon decomposition.

The third and commonly held explanation is that the enrichment of $\delta^{13}C$ with depth resulted from isotopic fractionation during the processes of microbial decomposition (Balesdent et al. 1993; Brunn et al. 2014; Campbell et al. 2009; Garten et al. 2000; Powers and Schlesinger 2002). Microbes always tend to utilize the lighter ^{12}C component and discriminate against heavier ^{13}C during SOM decomposition, and subsequently, the

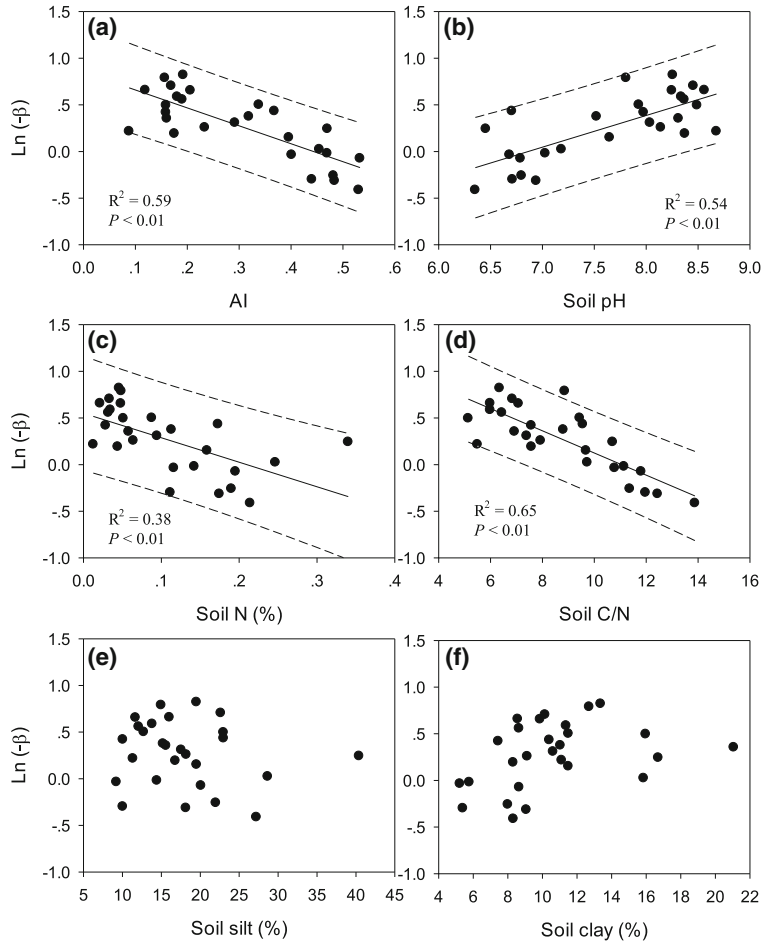

Fig. 2 Relationships between ln(−β) and aridity index (AI) and edaphic factors (Soil pH, N, C/N, silt and clay)

residual SOM becomes more enriched in ^{13}C (Diochon and Kellman 2008). If microbial isotopic fractionation is the dominate mechanism for $\delta^{13}C$ enrichment along depth profile, this increasing trend of soil $\delta^{13}C$ then can be used as an indicator of soil C turnover dynamics (Acton et al. 2013; Garten et al. 2000; Powers and Schlesinger 2002). We found the decomposition rate constant (k) was highly correlated with β value (Fig. 1), supporting our hypothesis (2) that carbon isotope ratios reflect soil carbon turnover processes and may be used as a reliable indicator for SOM decomposition rate. Of course, due to the complexity of the controlling factors on β value, β value should be used with caution, especially when C_4 plants do exist or have existed historically.

We also found that climatic and edaphic variables were correlated to β values, which is consistent with our

Table 2 Partial correlations between $\delta^{13}C$ / ln(−β) responses and aridity index (AI). Changes of correlations between $\delta^{13}C$ / ln(−β) responses and AI were controlled by each edaphic variable separately and all edaphic variables (column 'All'). Zero-order was the correlation between $\delta^{13}C$ / ln(−β) responses and AI including interactions with all geochemical variables. Differences between zero-order and partial correlations indicate the level of dependency of the $\delta^{13}C$ / ln(−β) responses on a given predictor. The color and numbers indicate the strength and sign of the correlation. The decrease and increase of color intensity means loss and gain of correlation, respectively; Clay (%); Silt (%); N (%); P, K, Ca, Mg, Fe, Mn, Zn, and Cu are in unit of mg per g dry soil.

	Aridity index (AI)														
	Zero-order	Clay	Silt	pH	CN	N	P	K	Ca	Mg	Fe	Mn	Zn	Cu	All
$\delta^{13}C$	-0.69	-0.67	-0.61	-0.27	-0.32	-0.22	-0.56	-0.67	-0.80	-0.60	-0.58	-0.68	-0.64	-0.51	0.18
ln(-β)	-0.79	-0.78	-0.80	-0.43	-0.18	-0.68	-0.76	-0.79	-0.80	-0.51	-0.62	-0.78	-0.74	-0.56	-0.18

hypothesis (3). Generally, climatic factors were considered as the primary controls in regulating β values (Acton et al. 2013; Garten et al. 2000; Yang et al. 2015). For example, Acton et al. (2013) compiled β values of 24 locations from published studies and revealed that β was dependent upon temperature across a range of cool temperate to tropical forest soils. In our arid grasslands, β value was also significantly correlated with aridity index (AI) as well as MAP and MAT (Fig. 2 and S6). However, the partial correlation analysis on climatic and edaphic factors showed that the correlations between β value and AI dropped significantly when edaphic factors were controlled (Table 2). The structure equation models (SEMs) also showed that AI indirectly affected β values through soil C/N ratio (Fig. 3). The negative correlation between β value and topsoil C/N ratio could be due to the faster microbial decomposition in soils with lower C/N ratio (Enríquez et al. 1993; Garten et al. 2000). Soil C/N ratio has often been associated inversely with the rate of SOM decomposition (Powers and Schlesinger 2002). Therefore, our results suggest that edaphic properties may play a more important role than climatic factors in β value and SOC decomposition. A recent study conducted along a 4000 km north-south transect of natural grassland and shrubland in Chile and the Antarctic Peninsula also showed that soil edaphic characteristics resulted from soil weathering directly controlled SOC dynamics in the long-term while climatic variables only acted largely as an influencing factor via governing soil weathering (Doetterl et al. 2015). Yang et al. (2015) found that edaphic (i.e. soil C/N ratio) rather than climatic variables (i.e. precipitation and temperature) were better explanations of $\delta^{13}C$ enrichment from vegetation to soil in Tibetan Plateau. In addition, Xu et al. (2016) used a data-assimilation approach and found that soil carbon decomposition rate is lower in soils with high soil C/N ratio. It should be noted that the C:N ratio of soil organic matter could be both a control of decomposition (SOM as substrate) and a result of decomposition (SOM as remainder of previous decomposition processes) and therefore its correlation with β value might not show causality. Nevertheless, our data provided evidence that soil substrate and chemical characteristics are more correlated with SOM decomposition and climatic factors might be indirect factors instead. Incorporation of both climatic and edaphic variables into Earth System Model could enhance the predictive power for addressing the spatial patterns of SOC storage and turnover, as well as for understanding future global responses of SOC to climate change.

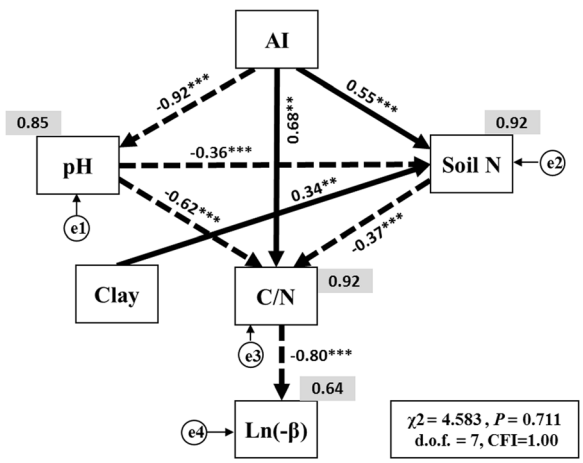

Fig. 3 The final structure equation models (SEMs) of the effects of climatic factors and edaphic variables on ln(−β). Measured variables are represented by boxes. Causal relationships are represented by one-headed arrows. Numbers adjacent to arrows are standardized path coefficients, analogous to relative regression weights, indicating the effect size of the relationship. Continuous and dashed black arrows indicate positive and negative relationship, respectively. * $p < 0.05$, ** $p < 0.01$, *** $p < 0.001$. χ^2, Chi-square; d.o.f, degrees of freedom; p: probability level; CFI: comparative fit index; nonsignificant χ^2 tests ($p > 0.05$) and CFI values over 0.90 are considered acceptable

Conclusion

We found soil $\delta^{13}C$ increased with soil depth along a large-scale transect in semi-arid grasslands. Results supported our hypothesis that this pattern was mainly driven by the microbial fractionation during decomposition and β value calculated from soil $\delta^{13}C$ and SOC concentration can be used as a good indicator for decomposition of SOC at large spatial scales. Aridity index (AI) combined with soil edaphic variables had the largest power in explaining β values. Soil C/N was correlated with the variations of β values while AI played an indirect role based on SEMs and partial correlation analysis, indicating that edaphic rather than climatic variables may be more important factors determining SOC decomposition in this region. Overall, despite some uncertainties associated with interpretation of soil $\delta^{13}C$ along its depth profile, our approach provides a fairly inexpensive way to study variations of SOC decomposition rate at large spatial scales.

Acknowledgements We thank two anonymous reviewers for useful comments on an earlier version of the manuscript. This work was financially supported by Major State Basic Research Development Program of China (973 Program, 2014CB954400), the National Natural Science Foundation of China (31522010 and 41601255), and Key Research Program of Frontier Sciences, CAS (QYZDB-SSWDQC006). We gratefully acknowledge all members of the Shenyang Sampling Campaign Team from the Institute of Applied Ecology, Chinese Academy of Sciences for their assistance during field sampling.

Reference

Accoe F, Boeckx P, Cleemput OV, Hofman G, Zhang Y, Guanxiong C (2002) Evolution of the $\delta^{13}C$ signature related to total carbon contents and carbon decomposition rate constants in a soil profile under grassland. Rapid Commun Mass Sp 16:2184–2189

Acton P, Fox J, Campbell E, Rowe H, Wilkinson M (2013) Carbon isotopes for estimating soil decomposition and physical mixing in well-drained forest soils. J Geophys Res Biogeosci 118: 1532–1545

Anderson JM (1991) The effects of climate change on decomposition processes in grassland and coniferous forests. Ecol Appl 1:326–347

Balesdent J, Girardin C, Mariotti A (1993) Site related ^{13}C of tree leaves and soil organic matter in a temperate Forest. Ecology 74:1713–1721

Bird MI, Chivas AR, Head J (1996) A latitudinal gradient in carbon turnover times in forest soils. Nature 381:143–146

Boström B, Comstedt D, Ekblad A (2007) Isotope fractionation and ^{13}C enrichment in soil profiles during the decomposition of soil organic matter. Oecologia 153:89–98

Brunn M, Spielvogel S, Sauer T, Oelmann Y (2014) Temperature and precipitation effects on $\delta^{13}C$ depth profiles in SOM under temperate beech forests. Geoderma 235-236:146–153

Campbell JE, Fox JF, Davis CM, Rowe HD, Thompson N (2009) Carbon and nitrogen isotopic measurements from southern Appalachian soils: assessing soil carbon sequestration under climate and land-use variation. J Environ Eng 135:439–448

Carvalhais N, Forkel M, Khomik M, Bellarby J, Jung M, Migliavacca M, Mu M, Saatchi S, Santoro M, Thurner M, Weber U, Ahrens B, Beer C, Cescatti A, Randerson JT, Reichstein M (2014) Global covariation of carbon turnover times with climate in terrestrial ecosystems. Nature 514:213–217

Delgado-Baquerizo M, Maestre FT, Gallardo A, Bowker MA, Wallenstein MD, Quero JL, Ochoa V, Gozalo B, García-Gómez M, Soliveres S (2013) Decoupling of soil nutrient cycles as a function of aridity in global drylands. Nature 502: 672–676

Desjardins T, Andreux F, Volkoff B, Cerri C (1994) Organic carbon and ^{13}C contents in soils and soil size-fractions, and their changes due to deforestation and pasture installation in eastern Amazonia. Geoderma 61:103–118

Dijkstra FA, Augustine DJ, Brewer P, von Fischer JC (2012) Nitrogen cycling and water pulses in semiarid grasslands: are microbial and plant processes temporally asynchronous? Oecologia 170:799–808

Diochon A, Kellman L (2008) Natural abundance measurements of ^{13}C indicate increased deep soil carbon mineralization after forest disturbance. Geophys Res Lett 35:L14402

Doetterl S, Stevens A, Six J, Merckx R, Van Oost K, Casanova Pinto M, Casanova-Katny A, Munoz C, Boudin M, Zagal Venegas E, Boeckx P (2015) Soil carbon storage controlled by interactions between geochemistry and climate. Nat Geosci 8:780–783

Ehleringer JR, Buchmann N, Flanagan LB (2000) Carbon isotope ratios in belowground carbon cycle processes. Ecol Appl 10: 412–422

Enríquez S, Duarte CM, Sand-Jensen K (1993) Patterns in decomposition rates among photosynthetic organisms: the importance of detritus C: N: P content. Oecologia 94:457–471

Feng J, Turner BL, Lü XT, Chen ZH, Wei K, Tian JH, Wang C, Luo WT, Chen LJ (2016) Phosphorus transformations along a large-scale climosequence in arid and semiarid grasslands of northern China. Global Biogeochem Cy 30:1264–1275

Flanagan LB, Brooks JR, Varney GT, Berry SC, Ehleringer JR (1996) Carbon isotope discrimination during photosynthesis and the isotope ratio of respired CO_2 in boreal forest ecosystems. Global Biogeochem Cy 10:629–640

Fontaine S, Barot S, Barré P, Bdioui N, Mary B, Rumpel C (2007) Stability of organic carbon in deep soil layers controlled by fresh carbon supply. Nature 450:277–280

Friedli H, Siegenthaler U, Rauber D, Oeschger H (1987) Measurements of concentration, $^{13}C/^{12}C$ and $^{18}O/^{16}O$ ratios of tropospheric carbon dioxide over Switzerland. Tellus B 39: 80–88

Garten CT, Hanson PJ (2006) Measured forest soil C stocks and estimated turnover times along an elevation gradient. Geoderma 136:342–352

Garten CT, Cooper LW, Post WM III, Hanson PJ (2000) Climate controls on forest soil C isotope ratios in the southern Appalachian Mountains. Ecology 81:1108–1119

Harris D, Horwáth WR, van Kessel C (2001) Acid fumigation of soils to remove carbonates prior to total organic carbon or carbon-13 isotopic analysis. Soil Sci Soc Am J 65:1853–1856

Hijmans RJ, Cameron SE, Parra JL, Jones PG, Jarvis A (2005) Very high resolution interpolated climate surfaces for global land areas. Int J Climatol 25:1965–1978

Kohl L, Laganière J, Edwards KA, Billings SA, Morrill PL, Van Biesen G, Ziegler SE (2015) Distinct fungal and bacterial $\delta^{13}C$ signatures as potential drivers of increasing $\delta^{13}C$ of soil organic matter with depth. Biogeochemistry 124:13–26

Lal R (2004) Carbon sequestration in dryland ecosystems. Environ Manag 33:528–544

Luo WT, Sardans J, Dijkstra FA, Peñuelas J, Lü XT, Wu HH, Li MH, Bai E, Wang ZW, Han XG, Jiang Y (2016) Thresholds in decoupled soil-plant elements under changing climatic conditions. Plant Soil 409:1–15

Nadelhoffer K, Fry B (1988) Controls on natural nitrogen-15 and carbon-13 abundances in forest soil organic matter. Soil Sci Soc Am J 52:1633–1640

Nielsen UN, Ball BA (2015) Impacts of altered precipitation regimes on soil communities and biogeochemistry in arid and semi-arid ecosystems. Glob Chang Biol 21:1407–1421

Poage MA, Feng XH (2004) A theoretical analysis of steady state $\delta^{13}C$ profiles of soil organic matter. Global Biogeochem Cy 18:GB2016. doi:10.1029/2003GB002195

Powers JS, Schlesinger WH (2002) Geographic and vertical patterns of stable carbon isotopes in tropical rain forest soils of Costa Rica. Geoderma 109:141–160

Reed SC, Coe KK, Sparks JP, Housman DC, Zelikova TJ, Belnap J (2012) Changes to dryland rainfall result in rapid moss mortality and altered soil fertility. Nat Clim Chang 2:752–755

Reynolds JF, Smith DMS, Lambin EF, Turner B, Mortimore M, Batterbury SP, Downing TE, Dowlatabadi H, Fernández RJ, Herrick JE (2007) Global desertification: building a science for dryland development. Science 316:847–851

Schweizer M, Fear J, Cadisch G (1999) Isotopic (^{13}C) fractionation during plant residue decomposition and its implications for soil organic matter studies. Rapid Commun Mass Sp 13:1284–1290

Staddon PL (2004) Carbon isotopes in functional soil ecology. Trends Ecol Evol 19:148–154

Torn MS, Lapenis AG, Timofeev A, Fischer ML, Babikov BV, Harden JW (2002) Organic carbon and carbon isotopes in modern and 100 year old soil archives of the Russian steppe. Glob Chang Biol 8:941–953

Wang C, Wang XB, Liu DW, Wu HH, Lü XT, Fang YT, Cheng WX, Luo WT, Jiang P, Shi J, Yin HQ, Zhou JZ, Han XG, Bai E (2014) Aridity threshold in controlling ecosystem nitrogen cycling in arid and semi-arid grasslands. Nat Commun 5:4799. doi:10.1038/ncomms5799

Wang C, Liu DW, Luo WT, Fang YT, Wang XB, Lü XT, Jiang Y, Han XG, Bai E (2016) Variations in leaf carbon isotope composition along an arid and semi-arid grassland transect in northern China. J Plant Ecol 9:576–585

Wynn JG, Harden JW, Fries TL (2006) Stable carbon isotope depth profiles and soil organic carbon dynamics in the lower Mississippi Basin. Geoderma 131:89–109

Xu X, Shi Z, Li D, Rey A, Ruan HH, Craine JM, Liang JY, Zhou JZ, Luo YQ (2016) Soil properties control decomposition of soil organic carbon: results from data-assimilation analysis. Geoderma 262:235–242

Yang YH, Ji CJ, Chen LY, Ding JZ, Cheng XL, Robinson D (2015) Edaphic rather than climatic controls over ^{13}C enrichment between soil and vegetation in alpine grasslands on the Tibetan plateau. Funct Ecol 29:839–848